ACS NANO

www.acsnano.org

ARTICLE

Direct Visualization of Vesicle Disassembly and Reassembly Using Photocleavable Dendrimers Elucidates Cargo Release Mechanisms

Shangda Li, Boao Xia, Bilal Javed, William D. Hasley, Adriel Melendez-Davila, Matthew Liu, Meir Kerzner, Shriya Agarwal, Qi Xiao, Paola Torre, Jessica G. Bermudez, Khosrow Rahimi, Nina Yu. Kostina, Martin Möller, Cesar Rodriguez-Emmenegger, Michael L. Klein, Virgil Percec,* and Matthew C. Good*

Cite This: https://dx.doi.org/10.1021/acsnano.0c02912

Read Online

ACCESS | Metrics & More | Article Recommendations | Supporting Information

ABSTRACT: Release of cargo molecules from cell-like nanocarriers can be achieved by chemical perturbations, including changes to pH and redox state and *via* optical modulation of membrane properties. However, little is known about the kinetics or products of vesicle breakdown due to limitations in real-time imaging at nanometer length scales. Using a library of 12 single−single type photocleavable amphiphilic Janus dendrimers, we developed a self-assembling light-responsive dendrimersome vesicle platform. A photocleavable *ortho*-nitrobenzyl inserted between the hydrophobic and hydrophilic dendrons of amphiphilic Janus dendrimers allowed for photocleavage and disassembly of their supramolecular assemblies. Distinct methods used to self-assemble amphiphilic Janus dendrimers produced either nanometer size small unilamellar vesicles or micron size giant multilamellar and onion-like dendrimersomes. *In situ* observation of giant photosensitive dendrimersomes *via* confocal microscopy elucidated rapid morphological transitions that accompany vesicle breakdown upon 405 nm laser illumination. Giant dendrimersomes displayed light-induced cleavage, disassembling and reassembling into much smaller vesicles at millisecond time scales. Additionally, photocleavable vesicles demonstrated rapid release of molecular and macromolecular cargos. These results guided our design of multilamellar particles to photorelease surface-attached proteins, photoinduce cargo recruitment, and photoconvert vesicle morphology. Real-time characterization of the breakdown and reassembly of lamellar structures provides insights on partial cargo retention and informs the design of versatile, optically regulated carriers for applications in nanoscience and synthetic biology.

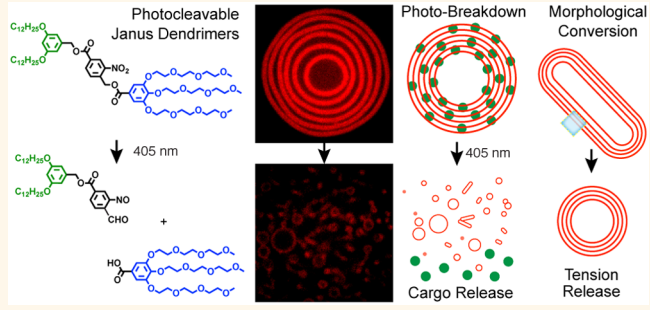

KEYWORDS: *photocleavable dendrimersomes, vesicle nanocarriers, cargo photorelease, multilamellar particles, photoconversion*

Unilamellar and multilamellar vesicles are supramolecular containers that have important applications as biomimetic cell-like compartments[1−5] and as nanocarriers in medicine,[6−11] food and agriculture,[12] and cosmetic technologies.[13] Synthetic vesicles, such as liposomes,[14−16] polymersomes,[17−19] and dendrimersomes,[20−24] provide versatile nanocarrier platforms for encapsulating cargos. Dendrimersomes additionally allow broad functionalization of their surfaces[25] for interactions with proteins, other vesicle carriers, and living cells.[26−28]

For many applications in nanoscience, the efficiency of loading into carriers and quantitative release of cargo are ultimate goals. However, visualization of the process of vesicle breakdown and product release remains challenging. Imaging of nanometer length scale vesicles requires electron microscopy, which does not allow for real-time characterization of

Received: April 6, 2020
Accepted: May 8, 2020
Published: May 8, 2020

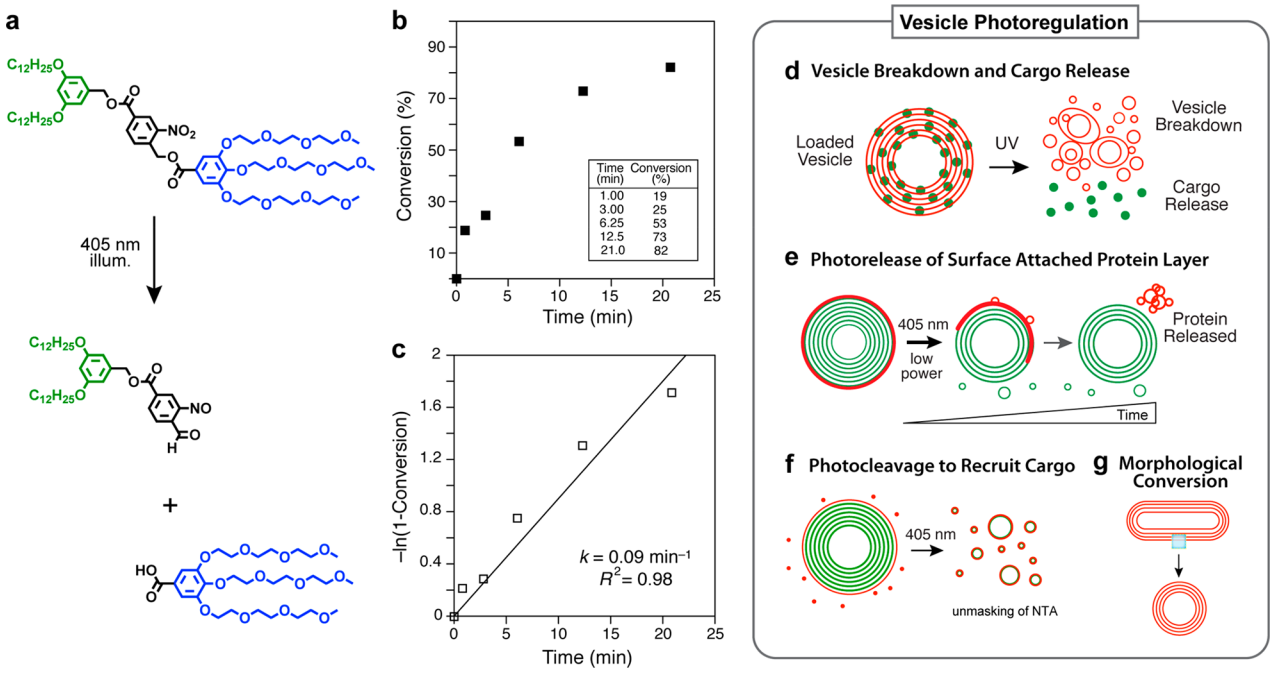

Figure 1. Photoresponsive dendrimersome vesicle platform. (a) Design of photocleavable amphiphilic Janus dendrimers containing a single NB unit between hydrophobic and hydrophilic dendrons. (b) Molecular cleavage of a photocleavage dendrimer as a function of illumination time using a mercury lamp with a DAPI filter. Conversion % monitored by product appearance on NMR. (c) Breakdown fits first-order kinetic reaction. (d–g) Strategies for vesicle photoregulation. (d) Schematic of vesicle breakdown and cargo release. (e) Strategy for photorelease of protein attached to outer lamellar layer at low power. (f) Photoinduced cargo recruitment: vesicle breakdown reveals attachment sites. (g) Morphological photoconversion of vesicle ultrastructure.

vesicle ultrastructure dynamics at millisecond time scales. Breakdown of vesicles can be induced *via* the incorporation of pH-responsive,[29−31] redox,[32−34] or light-responsive[35−42] units in the membrane of nanocarriers, and release measured by biochemical assays.[20,37−42] In the case of optically triggered cargo release,[42] strategies have included photochemical cleavage of chemical bonds[37−40] or *cis*−*trans* isomerization of azobenzene to change bilayer packing.[41] However, at low-power UV irradiation, cargo release kinetics are limited by the rate of vesicle breakdown, which can be slow. Furthermore, the cleavage products of giant vesicles including dendrimersomes have not been investigated.[37]

Previous work from our laboratory elaborated twin−twin,[20,43] single−single,[44] and sequence-defined[45−47] amphiphilic Janus dendrimers and glycodendrimers. These amphiphiles self-assemble by injection in water or thin-film hydration to form stable dendrimersomes and glycodendrimersomes that readily encapsulate hydrophobic and hydrophilic molecules.[25] Their stability and dynamic membranes make dendrimersomes capable of forming cell-like hybrids with both bacterial[26] and human cell membranes[27] and engulfing living bacteria *via* endocytosis.[28] Their exteriors can be decorated with proteins and nucleic acid,[25] and glycodendrimersomes have been used to generate surface nanostructures for elucidating features of protein−glycan interactions on a biomimetic synthetic cell membrane.[45,48] We reasoned that the chemical flexibility of these dendrimer amphiphiles would provide an ideal platform for generating a photoresponsive vesicle platform.

In this study, a library of 12 single−single type[44] photocleavable amphiphilic Janus dendrimers was designed and synthesized to create photocleavable dendrimersome compartments (Figure 1). The *ortho*-nitrobenzyl (NB) group[49−51] was used as a photolabile unit between the hydrophobic and hydrophilic dendrons of the amphiphilic Janus dendrimers (Figure 1a), and the molecular products of dendrimer photocleavage were measured by NMR (Figure 1b,c). A majority of members of the library of Janus dendrimers self-assembled into photoactive vesicles (Figure 1d), including unilamellar and multilamellar, onion-like dendendrimersomes and other complex supramolecular architectures. Illumination *via* 405 nm laser and confocal imaging of giant dendrimersomes *in situ* enables direct observation of vesicle breakdown and lamellar reassembly. Following milliseconds to seconds of illumination, dendrimersomes photocleaved, disassembled, and reassembled into smaller vesicles and tubular structures (Figure 1d). When preloaded with cargo, these dendrimersomes released up to 75−90% of their molecular or macromolecular cargos following seconds of illumination. This effect was specific because control dendrimersomes lacking a photocleavable group did not break down or release their cargo. We further designed multifaceted strategies for optical modulation, including photorelease of proteins bound to the vesicle surface (Figure 1e), optical cargo recruitment (Figure 1f), and conversion of vesicle morphology (Figure 1g).

RESULTS AND DISCUSSION

Synthesis of Photocleavable Amphiphilic Janus Dendrimers. In contrast to the incorporation of multiple photocleavable units in the hydrophobic branches of Janus dendrimers,[37] single−single photocleavable amphiphilic Janus dendrimers were designed with 12 AB_3 and constitutional isomeric AB_2 hydrophobic dendrons and with AB_3 hydrophilic dendrons.[20,21,44] The photocleavable unit, NB group,[49−51] bridges the hydrophobic minidendron to the hydrophilic one (Figure 1a). In principle, the NB group can be cleaved by

https://dx.doi.org/10.1021/acsnano.0c02912
ACS Nano XXXX, XXX, XXX−XXX

Scheme 1. Synthesis of hydrophobic dendrons.[a]

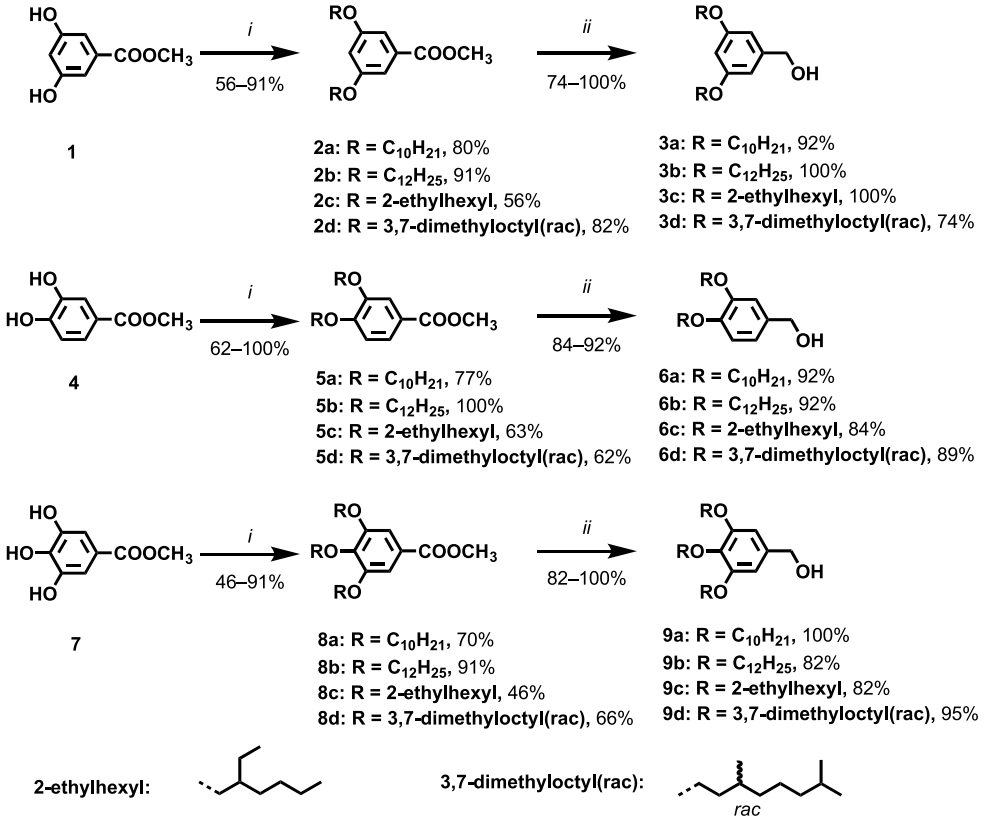

[a]Reagents and conditions: (i) RBr, K_2CO_3, DMF, 120 °C, 4 h; (ii) $LiAlH_4$, THF, 0–23 °C, 1 h.

Scheme 2. Synthesis of hydrophobic dendrons containing *ortho*-nitrobenyl (NB) units[a]

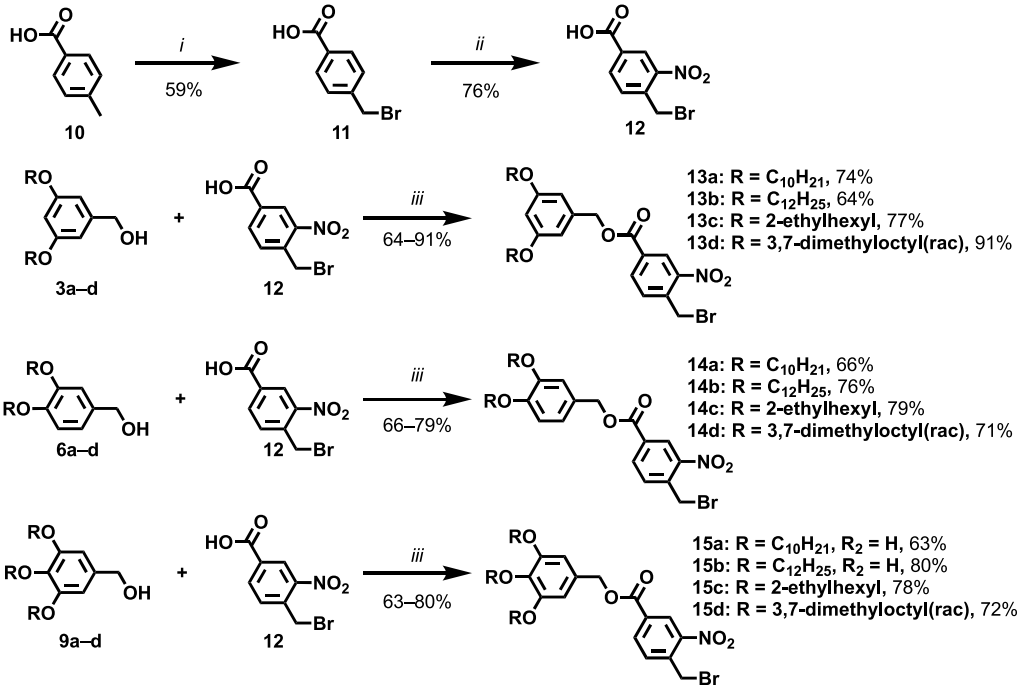

[a]Reagents and conditions: (i) NBS, BPO, $CHCl_3$, 65 °C, 16 h. (ii) fuming HNO_3, −10 °C, 2.5 h. (iii) DCC, DPTS, DCM, 23 °C, 16 h.

ultraviolet light to generate an aldehyde with the hydrophobic minidendron with an acid containing the hydrophilic dendron (Figure 1a).[49−51]

Twelve esters of hydrophobic AB_3 and constitutional AB_2 minidendrons (**2a−d**, **5a−d**, and **8a−d**) were synthesized orthogonally *via* an optimized Williamson etherification from

https://dx.doi.org/10.1021/acsnano.0c02912
ACS Nano XXXX, XXX, XXX−XXX

Scheme 3. Synthesis of Libraries of Photocleavable Janus Dendrimers[a]

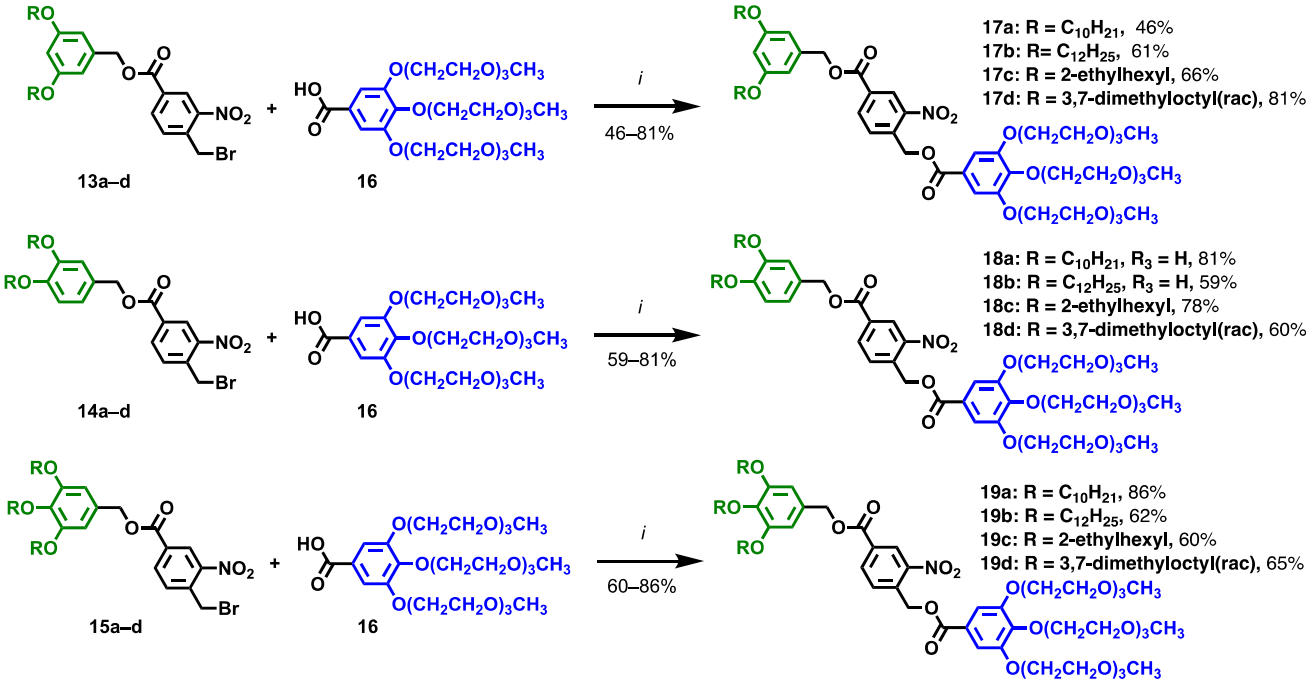

[a]Reagents and conditions: (i) $NaHCO_3$, DMF, 40 °C, 16 h.

four alkyl bromides (RBr) including *n*-decyl bromide, *n*-dodecyl bromide, branched 2-ethylhexyl bromide, and racemic branched 3,7-dimethyloctyl bromides with methyl 3,5-dihydroxybenzoate (**1**), methyl 3,4-dihydroxybenzoate (**4**), and methyl 3,4,5-trihydroxybenzoate (**7**) (Scheme 1). Their reduction by $LiAlH_4$ in tetrahydrofuran (THF) gave the corresponding hydrophobic minidendron alcohols (**3a–d**, **6a–d**, and **9a–d**) in 70–100% yields.

A bifunctional molecule containing NB unit 4-(bromomethyl)-3-nitrobenzoic acid (**12**) was synthesized according to a literature procedure (Scheme 2).[52] The commercially available 4-methylbenzoic acid (**10**) was selectively monobrominated by *N*-bromosuccinimide (NBS) on its methyl group *via* a radical mechanism mediated by benzoyl peroxide (BPO) in chloroform to obtain 4-(bromomethyl)benzoic acid (**11**) in 59% yield.[52] Nitration of 4-(bromomethyl)benzoic acid with fuming HNO_3 gave 4-(bromomethyl)-3-nitrobenzoic acid (**12**) in 76% yield.[51,52] 4-(Bromomethyl)-3-nitrobenzoic acid (**12**) was reacted with the alcohols **3a–d**, **6a–d**, and **9a–d** under mild esterification conditions with *N*,*N*′-dicyclohexylcarbodiimide (DCC) in the presence of 4-(dimethylamino)pyridinium 4-toluenesulfonate (DPTS) to generate the corresponding esters **13a–d**, **14a–d**, and **15a–d** containing active bromomethyl units.

Finally, a very mild Williamson etherification in the presence of $NaHCO_3$ at 40 °C between the esters **13a–d**, **14a–d**, and **15a–d** with the active bromomethyl units and 3,4,5-tris(2-(2-(2-methoxyethoxy)ethoxy)ethoxy)benzoic acid (**16**) was successfully applied to obtain the 12 target photocleavable amphiphilic Janus dendrimers **17a–d**, **18a–d**, and **19a–d** containing NB units, with a range of yields from 46% to 86% (Scheme 3). Among these photocleavable amphiphilic Janus dendrimers, **17**, **18**, and **19** correspond to their constitutional isomeric AB_2 3,5-, 3,4-, and AB_3 3,4,5-substitued alkyl benzoic ester on their hydrophobic dendron part, and **a**, **b**, **c**, and **d** correspond to *n*-decyl, *n*-dodecyl, branched 2-ethylhexyl, and racemic branched 3,7-dimethylocty chains. To easily recognize their molecular structures, the nomenclature for all the photocleavable Janus dendrimers (Figure 2a and Figure 3a) was also provided by following the rules developed by our laboratory.[20,21] For example, **17b: (3,5)12G1-NB-(3,4,5)3EOG1** means that the molecule has a 3,5-didodecyoxyl benzoic minidendron [(3,4,5)12G1, G1 denotes a first-generation dendron] in its hydrophobic part, a 3,4,5-tris(2-(2-(2-methoxyethoxy)ethoxy)ethoxy)benzoic [(3,4,5)3EOG1] in its hydrophilic part, and an NB unit connecting these two parts.

Photocleavage of Dissolved Janus Dendrimer Molecules. To monitor the photocleavage reaction of Janus dendrimers (Figure S1), we used a variety of analytic methods, including NMR, LC-MS, and MALDI-TOF. Photocleavage reactant and products are detectable *via* NMR (Figure S2a), confirming the proposed mechanism. Kinetics of photocleavage of the **17b: (3,5)12G1-NB-(3,4,5)3EOG1** dendrimer was monitored by NMR, and half-cleavage was achieved in a matter of minutes using a focused mercury lamp and a DAPI filter (Figure 1a,b). Kinetics could also be monitored for standard overhead illumination *via* a 365 nm UV lamp (Figure S2b,c). Additionally, photocleavage products were confirmed and monitored by MALDI-TOF (Figure S3) and LC-MS (Figures S4, S5).

Self-Assembly of Nanoscale Dendrimersome Vesicles by Injection. Nanoscale self-assemblies of photocleavable amphiphilic Janus dendrimers were prepared by injection of a THF solution containing a dendrimer into water. These vesicles were subsequently characterized by dynamic light scattering (DLS) and cryogenic transmission electron microscopy (cryo-TEM) (Figure 2 and Figure S1). Janus dendrimers with 3,5- or 3,4-substituted hydrophobic dendrons with linear *n*-decyl or *n*-dodecyl chains had a narrow polydispersity in DLS (PDI lower than 0.3) (Figure 2a). Representative cryo-TEM images showed that Janus dendrimers with 3,5-substituted

https://dx.doi.org/10.1021/acsnano.0c02912
ACS Nano XXXX, XXX, XXX–XXX

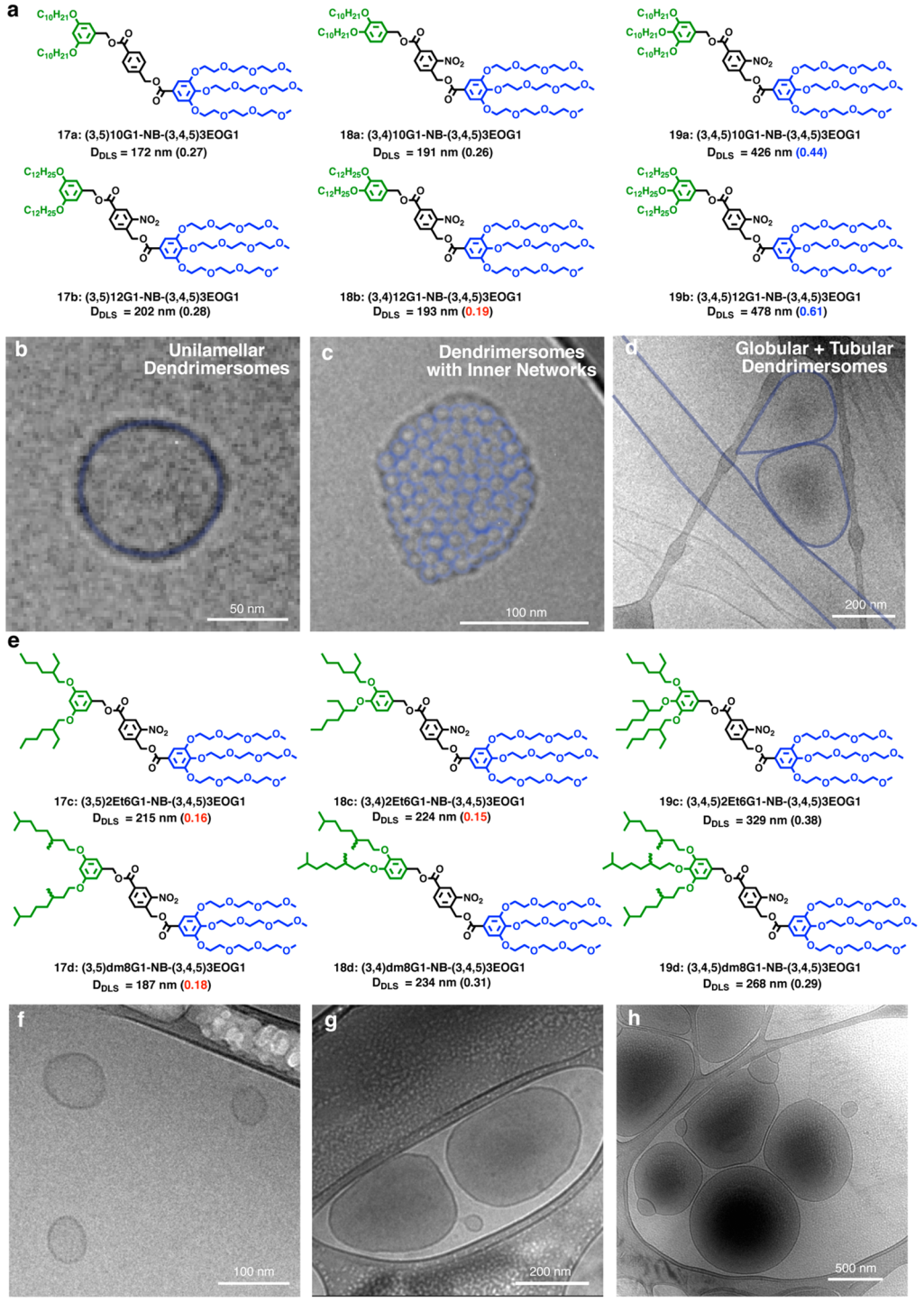

Figure 2. Library of photocleavable dendrimers and visualization of the structure of self-assembled nanovesicles formed by injection *via* cryo-TEM. (a) Chemical structures of photocleavable Janus dendrimers with linear decyl or dodecyl chains containing an NB linker, assembled by injecting a THF solution containing them into water (0.5 mg/mL). *Z*-average diameters (D_{DLS}), an intensity value, and polydispersities (in parentheses; color code: red, narrow; blue, broad; black: moderate) (b–d) Representative cryo-TEM images of self-assembled dendrimersomes at 1.0 mg/mL: (b) unilamellar dendrimersomes; typical image for 17a and 17b; (c) dendrimersomes with inner networks; typical image for 18a and 19a; (d) mixtures of globular dendrimersomes and tubular dendrimersomes; typical image for 19b. Red tracing indicates electron-dense regions. (e) Chemical structures of photocleavable Janus dendrimers with branched 2-ethylhexyl or racemic 3,7-dimethyloctyl chains containing an NB linker, assembled by injection. Diameters (D_{DLS}) and polydispersities obtained at a 0.5 mg/mL final concentration. (f–h) Selected cryo-TEM of self-assembled unilamellar dendrimersomes: (f) small size unilamellar dendrimersomes; typical image for 17c, 17b, 18c, and 18d, (g) medium size unilamellar dendrimersomes; typical image for 19c, and (h) large size unilamellar dendrimersomes; typical image for 19d. Larger diameters are obtained at concentrations higher than 0.5 mg/mL.

dendrons tended to assemble into vesicular dendrimersomes (Figure 2b). Janus dendrimers with 3,4- and 3,4,5-*n*-decyl-substituted dendrons often assembled into dendrimersomes with inner networks (Figure 2c). Janus dendrimers **18b** and

https://dx.doi.org/10.1021/acsnano.0c02912
ACS Nano XXXX, XXX, XXX–XXX

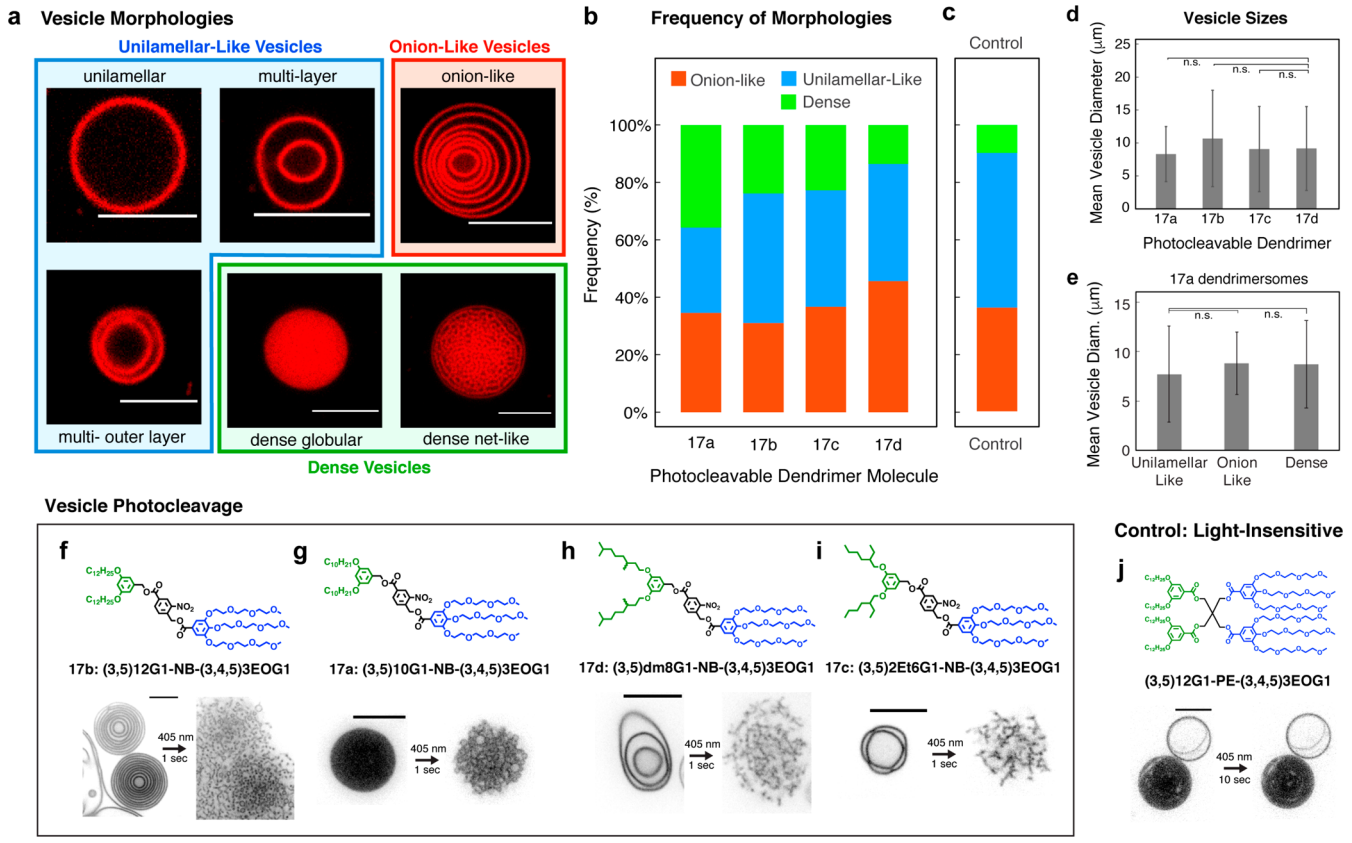

Figure 3. Self-assembly of giant dendrimersomes, morphologies, and imaging of vesicle photocleavage. (a) Giant vesicles formed by hydration achieved characteristic morphologies and sizes. Shape types observed included unilamellar-like vesicles with ≤2 visible layers) (blue), onion-like multilayer vesicles (red), and dense vesicles (green). Dendrimersomes labeled with (3,5)12G1-RhB (0.2% w/w) was used during film hydration for fluorescence microscopy. Scale bar is 10 μm. (b) Frequency of observing distinct types of vesicle morphology for four photocleavable dendrimers: 17a–d; *n* > 90 vesicles per sample. (c) distribution of vesicle morphologies for control dendrimers (3,5)10G1-PE-(3,4,5)3EOG1. (d) Mean and standard deviation of vesicle diameters formed *via* thin-film hydration. The differences in the mean diameters are not statistically significant (n.s.). (e) Means and standard deviation of vesicle diameters for shape classes of vesicles for the 17a dendrimer. Differences in mean vesicle sizes were not statistically significant (f–i) Photocleavage of giant vesicles upon 1 s of 405 nm laser illumination. Representative images of light-triggered vesicle breakdown for photosensitive dendrimers (f) 17b, (g) 17a, (h) 17d, and (i) 17c show breakdown of all three types of vesicle morphologies. (j) Control dendrimer (3,5)12G1-PE-(3,4,5)3EOG1 does not disassemble in response to 10 s of 405 nm illumination. Scale bar is 10 μm.

19b self-assembled into a mixture of morphologies, including globular and tubular dendrimersomes (Figure 2d). Janus dendrimers containing branched 2-ethylhexyl or racemic branched 3,7-dimethyl chains on their hydrophobic dendrons had a narrower PDI compared to their linear chain analogues (Figure 2e). All of them self-assembled into uniform vesicular dendrimersomes whose dimensions depend on the concentration (Figure 2f–h).[21,44] These results suggest that the branched alkyl chains may prevent the formation of more organized assemblies such as onion-like dendrimersomes.

UV-Mediated Breakdown of Nanoscale Dendrimersomes. Light-responsive nanoscale dendrimersome vesicles were self-assembled by injection of **17b: (3,5)12G1-NB-(3,4,5)-3EOG1** in THF solvent into water. After assembly, vesicles were illuminated for 30 min using a 365 nm UV lamp and imaged *via* cryo-TEM. Electron microscopy revealed that after prolonged irradiation the photocleavable dendrimersomes evolved to dense structures or were broken down into vesicles much smaller in size and aggregates (Figure S2). Dendrimer cleavage results in two dendrons: a hydrophilic one, readily soluble in water, and the insoluble hydrophobic one, whose aggregation is observable *via* cryo-TEM. Such hydrophobic aggregates could provide a reservoir to reassemble small vesicles from uncleaved amphiphiles or contribute to retention of loaded cargos. One challenge with this approach is that we could not track the dynamics of optically mediated vesicle disassembly or image the direct breakdown products of the same vesicle before and after illumination. Therefore, we turned to real-time imaging of giant vesicles using fluorescence microscopy.

Self-Assembly and Photocleavage of Giant Dendrimersomes. A useful feature of thin-film vesicle rehydration is formation of cell-sized particles that display a diverse range of structural morphologies.[53,54] Unlike nanoscale vesicles formed by injection, the morphologies of hydrated giant vesicles are more varied. However, the sizes and broad diversity of shapes provide an excellent opportunity to characterize the photoresponsiveness of an assortment of vesicles' ultrastructures. Importantly, the micron sizes of these giant vesicles formed by hydration enable real-time imaging of lamellar dynamics on a fluorescence microscope.[55]

To characterize the dynamic, light-induced breakdown of photosensitive dendrimersomes, giant vesicles were formed by thin-film hydration at 50 °C on a Teflon sheet in water.[20,25] To enable fluorescence imaging *via* confocal microscopy *in situ*, a tracer, rhodamine B red-fluorescent-labeled Janus dendrimer

https://dx.doi.org/10.1021/acsnano.0c02912
ACS Nano XXXX, XXX, XXX–XXX

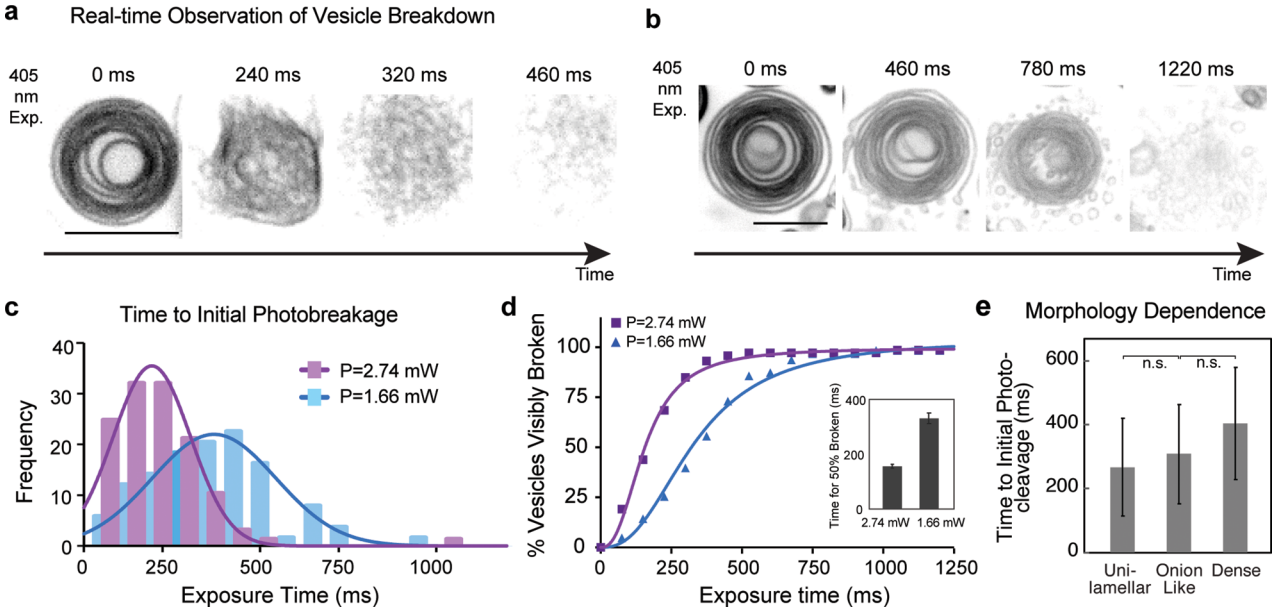

Figure 4. Kinetics of light-induced vesicle breakdown observed in real time. (a, b) Dendrimer 17a photocleavage *via* 405 nm laser illumination leads to vesicle disassembly in millisecond time scales: (a) power 2.74 mW, (b) power 1.66 mW. (c) Distribution of times required to observe initial lamellar breaking—defined as duration of 405 nm exposure required to first observe breaks in dendrimersome lamellae from confocal microscopy images—displays a laser power dependence. Gaussian fit: Mean: 193 ms at 2.74 mW power (n = 73 vesicles) and 370 ms at 1.66 mW power (n = 63 vesicles). Distributions differ significantly: p-value < 0.0001. Scale bar is 10 μm. (d) Cumulative frequency distribution for photobreakage upon 405 nm exposure time. Cumulative Gaussian fit. Inset time to generate initial breaks in 50% of vesicles. (e) Average time to initial photocleavage for three morphological types of vesicles: unilamellar-like, onion-like, and dense for 2.74 mW laser power. Standard deviation from mean. Not statistically significant (n.s.). Scale bar is 10 μm.

(3,5)12G1-RhB, was included (Figure S9a).[25,56] The giant dendrimersomes hydrated from photocleavable Janus dendrimers typically self-assembled to a vesicle diameter of 5−10 μm, achieving one of a reproducible subset of morphologies (Figure 3a). Unilamellar-like vesicles containing two or fewer visible layers, multilamellar onion-like[25,46,57] and dense or net-like dendrimersomes, were regularly observed. The frequency of these morphologies among vesicles self-assembled from four distinct photocleavable dendrimers was similar (Figure 3b) and similar to vesicles assembled from control dendrimers (Figure 3c). Further, the average sizes of vesicle observed *via* thin-film hydration were statistically indistinguishable (Figure 3d). And even among the different types of morphologies, vesicles often assembled to a similar size (Figure 3e). Overall, we did not observe a photocleavable dendrimer that predominantly formed only one morphological class of vesicles. Instead, a diverse set of vesicle morphologies, of relatively similar sizes, was accessible with each dendrimer molecule.

Photocleavable dendrimers self-assembled into giant dendrimersomes that readily disassembled in response to a 1 s pulse of a 405 nm laser at 1.66 mW. Illumination of vesicles formed by photocleavable dendrimers **17a**, **17b**, **17c**, and **17d** led to rapid vesicle disassembly (Figure 3f−i). Light-regulated disassembly occurred for four types of dendrimersomes and three morphological classes of vesicles. Importantly, a control experiment using photoinsensitive Janus dendrimer **(3,5)12G1-PE-(3,4,5)-3EOG1**, containing a pentaerythritol (PE) core,[20,25] demonstrated that the laser power and exposure times used in our experiments do not nonspecifically ablate standard dendrimersomes (Figures 3j, S9a,b). Therefore, photocleavage is selective. LC-MS analysis of photocleavage shows identical products, regardless of whether illumination is performed on dendrimer molecules or preassembled vesicles, validating our strategy (Figure S8). Debris from photocleavage was visibly present (Figure 3b−e), leading to re-formation of small dendrimer vesicles (Figure S9c), although some of the objects are likely smaller than the resolution of the microscope (<280 nm).

Kinetics of Light-Mediated Vesicle Breakdown. To observe real-time optical disassembly of dendrimersome vesicles, we shortened the illumination to 20 ms pulses and collected image time courses as a function of a 405 nm exposure time. We observed initial vesicle photobreakage—defined as the duration of 405 nm exposure required to visually observe first breaks within the lamellae from confocal microscopy images—within tens to hundreds of milliseconds (Figures 4a,b and S10 and supplemental movies 1−4) and near complete breakdown within seconds. The average time to observation of initial breaks in lamellae was dependent on laser power and varied between 193 and 370 ms (Figure 4c). Within that duration, more than half of vesicles displayed visible breaks to the lamellae (Figure 4d). At higher power, greater than 90% of vesicles displayed initial photobreakage within 400 ms. The morphology of the vesicle had a small impact on photosensitivity: unilamellar vesicles were slightly more labile than onion-like vesicles, which in turn broke more quickly than dense vesicles (Figure 4e); however these differences were not statistically significant. Altogether, this *in situ* imaging reveals the rapid breakdown kinetics achievable using photocleavable dendrimer vesicles when the illumination source is not the rate-limiting step to vesicle disassembly and demonstrates the real-time optical disassembly of a variety of distinct vesicle morphologies.

Cargo Release from Photoactive Dendrimersomes. To characterize the functionality of our photosensitive dendrimesomes as carriers, we first loaded them with small-

https://dx.doi.org/10.1021/acsnano.0c02912
ACS Nano XXXX, XXX, XXX−XXX

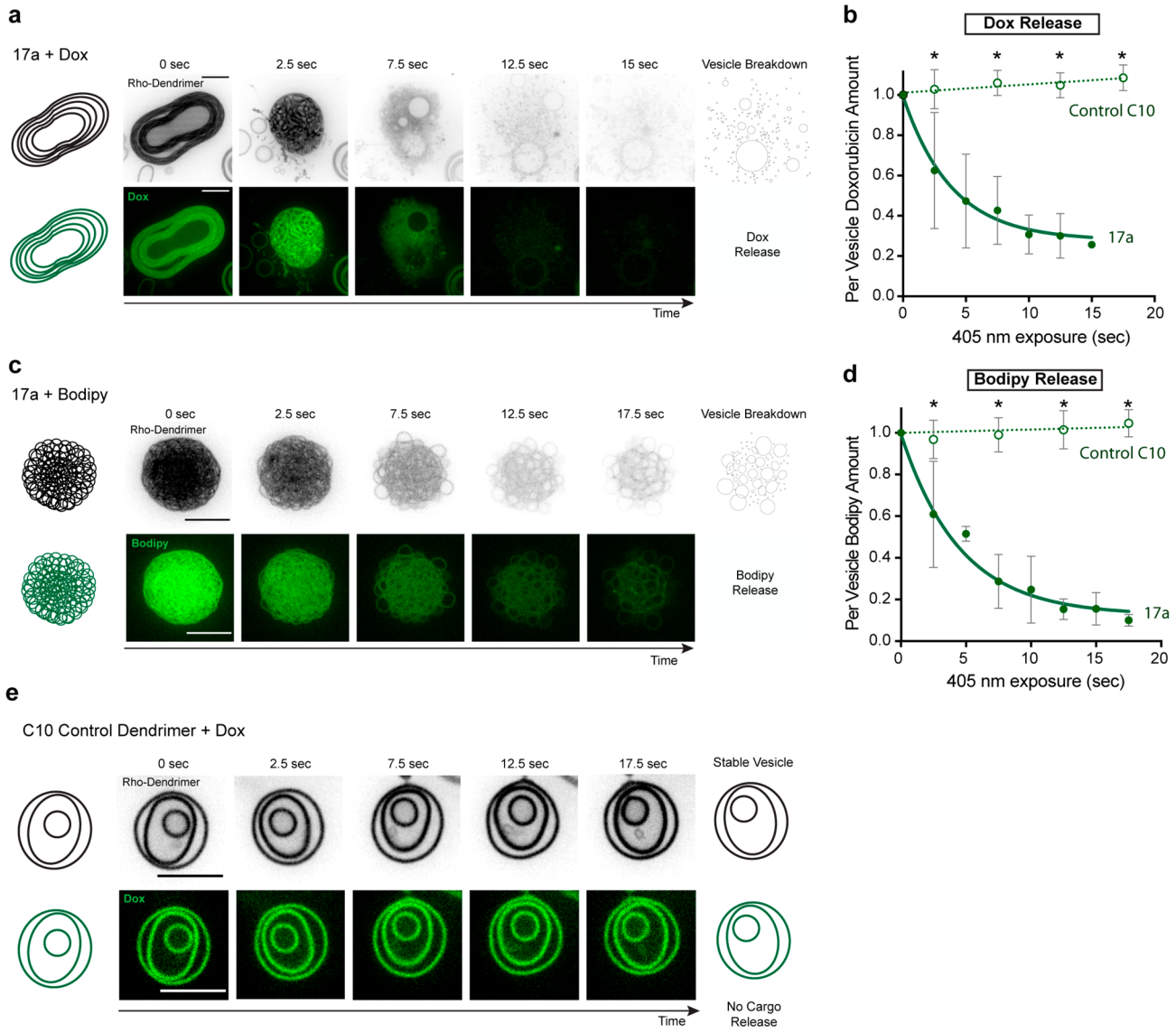

Figure 5. Dose-dependent, optically controlled cargo release from multilayer dendrimer vesicles. (a) Vesicle breakdown and doxorubicin cargo release. (b) Quantitation of doxorubicin release—measured by imaging of fluorescent cargo retained in the vesicle—from photosensitive and control dendrimersomes as a function of 405 nm exposure time. (c) Vesicle breakdown and release of a hydrophobic molecule, Bodipy. (d) Quantitation of Bodipy release. (e) Control dendrimersomes are insensitive to 405 nm laser exposure: they do not break down or photobleach. Error bars: standard deviation from mean. n > 20 vesicles for 17a and n > 10 vesicles for control dendrimers. 17a data fit to first-order exponential decay and control data fit linearly. *p-values < 0.001 comparing control *versus* photocleavable dendrimersomes at indicated time points. Scale bar is 10 μm.

molecule cargos. The drug doxorubicin and hydrophobic small molecule Bodipy are green fluorescent low molecular weight molecules readily encapsulated in giant dendrimersome vesicles.[25] Upon 405 nm illumination, we observed small-molecule cargo release concomitant with vesicle disassembly (Figure 5a–d). Release was dependent on the dose of light, and photocleavable dendrimersomes released 70–85% of their cargo within 15 s (Figure 5b,d). Multiple members of the photocleavable dendrimer library showed photoinduced cargo release (Figure S11a–f). Control dendrimersomes that lack photocleavable groups were insensitive to illumination: they did not break down and showed no photobleaching of **(3,5)12G1-RhB** dendrimer tracer or cargos over 20 s of 405 nm illumination (Figure 5e, Figure S11g,h). Retention of a fraction of initial cargo upon photoinduced disassembly is likely due to the presence and spontaneous re-formation of breakdown products into small lamellar structures.

Next, we investigated the photorelease of macromolecular cargo, such as enzymes, encapsulated in giant dendrimersome vesicles. *E. coli* dihydrofolate reductase (DHFR)[58] fused to GFP was loaded during the vesicle hydration step and accumulated in giant dendrimersomes (Figure S12a). Similar to small-molecule release, 405 nm illumination triggered vesicle breakdown and enzyme release from photocleavable but not control dendrimersomes (Figure S12b–d). These results demonstrate the feasibility of photoreleasing proteins and enzymes, offering a tool to interface with and modulate cells in response to light stimuli for synthetic biology.

Optical Strategies to Selectively Release or Recruit Macromolecular Cargos. Multilamellar dendrimersomes[25,46,57] offer a multitude of regulatory handles for

https://dx.doi.org/10.1021/acsnano.0c02912
ACS Nano XXXX, XXX, XXX–XXX

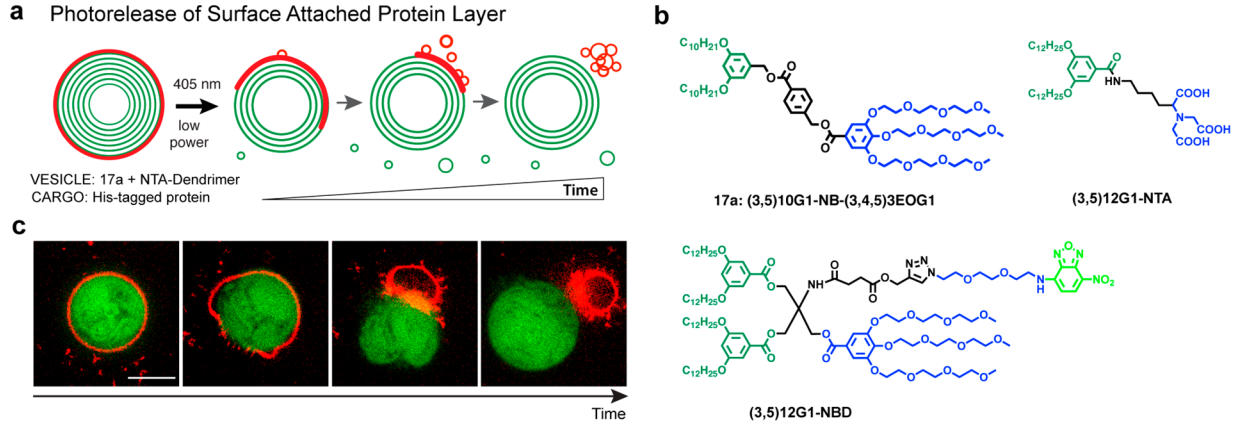

Figure 6. Light-induced release of attached protein cargo from core−shell particle architectures. (a) Schematic of surface-attached protein release from vesicle exterior at short exposure times. (b) Molecular structures: NTA-dendrimer binds His-tagged protein; NBD-dendrimer used as green fluorescent tracer.[59] (c) Photorelease of His6-RFP protein from vesicle exterior. Scale bar is 10 μm.

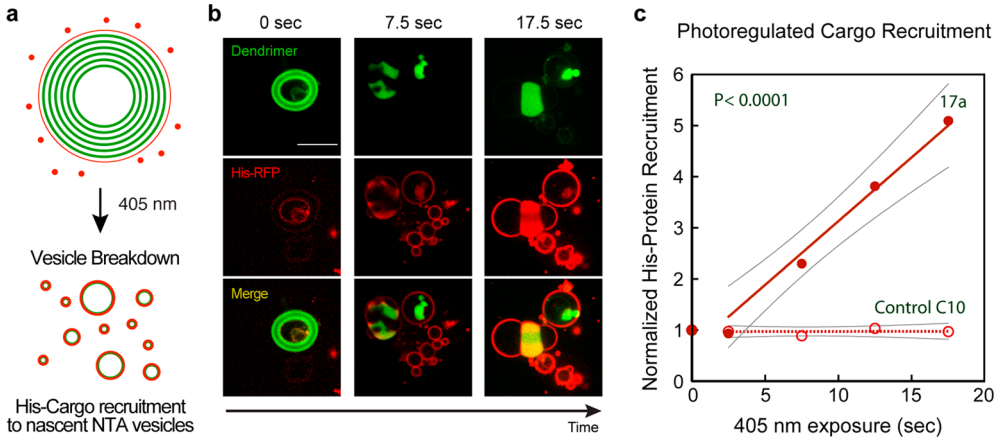

Figure 7. Protein photorecruitment upon vesicle breakdown. (a) Schematic of light-induced vesicle breakdown to reveal NTA dendrimer and recruit exogenous cargo protein. (b) Images of vesicle photocleavage causing formation of small nascent vesicles that rapidly recruit His-RFP. (c) Quantitation of selective cargo recruitment upon photomediated dendrimersome disassembly. Linear regression showing 95% confidence interval fit to data from 2.5 to 17.5 s. Slopes differ significantly: p-value < 0.0001. n = 23 vesicles (17a) and n = 11 vesicles (control). Scale bar is 10 μm.

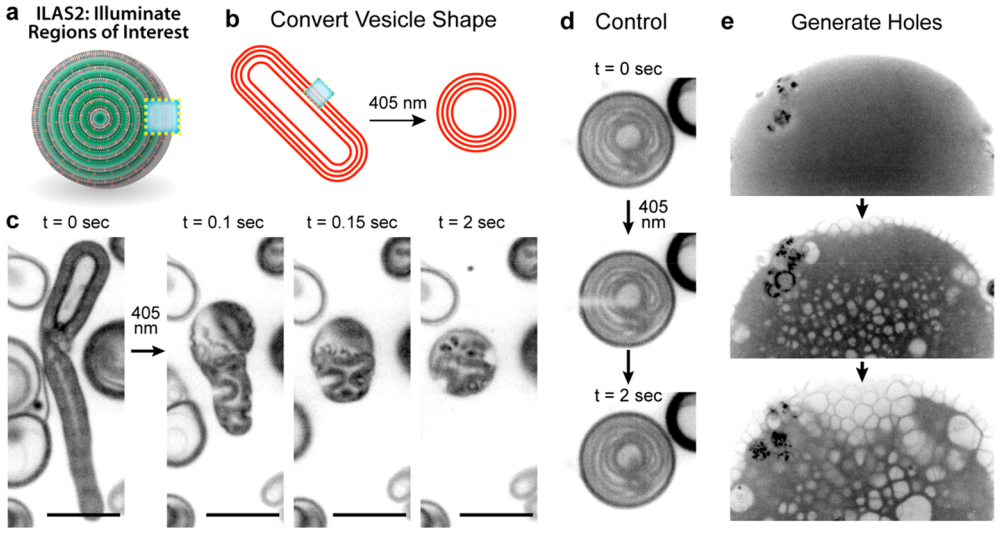

Figure 8. Triggerable morphological conversion of photocleavable dendrimersomes. (a) Schematic: micropoint laser illumination of a small region of interest. (b) Morphology of vesicles can be altered in response to 405 nm illumination. (c) Illumination of a small region leads to rapid conversion of a vesicle from tubular to spherical shape. (d) Control dendrimersomes are insensitive to similar illumination of a box across the midpoint of the vesicle. (e) Dense vesicles display generation and growth of holes upon illumination. Scale bar is 10 μm.

https://dx.doi.org/10.1021/acsnano.0c02912
ACS Nano XXXX, XXX, XXX−XXX

optically controlled recruitment and release of protein components. Their lamellae can be photocleaved to release encapsulated components (Figures 5, S12). Additionally, the internal layers of performed dendrimersome particles are largely impermeant to macromolecules added in solution, and their outer layers can be functionalized with moieties such as nitrilotriacetic acid (NTA) to selectively recruit histidine-tagged proteins (Figure 6a).[25] Hydration of photocleavable vesicles in the presence of 4% **(3,5)12G1-NTA** (Figure 6b) facilitated the surface recruitment of a His-tagged red fluorescent protein (His-RFP) to the dendrimersome exterior (Figure 6). Upon low doses of 405 nm illumination (<1 s), we observed breakage and rapid release of the outer vesicle layer, thereby liberating the cargo from the dendrimersome particle (Figures 6c, S13a). Control vesicles did not release surface-attached cargo (Figure S13b).

Next, we tested the feasibility of photomediated cargo recruitment. In stable multilamellar dendrimersomes, the internal lamellae are largely inaccessible to proteins present in solution. We hypothesized that photomediated breakdown of NTA-decorated dendrimersomes would generate nascent NTA vesicles capable of binding to His-tagged protein (Figure 7a). Indeed we observed strong light-induced recruitment of His-RFP to vesicles produced from photocleavage of the initial carrier (Figure 7b,c). Altogether, this versatile platform provides a system to inducibly sequester protein from the surrounding environment for remediation or to rapidly optically trigger the release internal or surface-attached cargos.

Finally, we observed a reproducible morphological phenomenon of vesicle shape conversion in response to light (Figure 8a,b). Pointed illumination of outer lamellar layers in elongated dendrimersomes led to rapid retraction and formation of spherical particles (Figure 8c, supplemental movies 5 and 6). Such localized illumination had no effect on control dendrimer vesicles, demonstrating that the laser power does not ablate normal vesicle lamellae (Figure 8d). Additionally, in some dense dendrimersome vesicle structures we observed steady hole formation and growth (Figure 8e), suggesting the mechanism by which photocleavable dendrimer vesicles change structure and break down.

CONCLUSIONS

A library of 12 photocleavable amphiphilic Janus dendrimers that self-assemble into light-responsive vesicles and real-time imaging of their disassembly, reassembly, and morphological conversion elucidated kinetics of cargo release and mechanisms of cargo retention. Direct imaging of the dynamics of vesicle breakdown, layer-by-layer release, and cargo binding is not feasible *via* cryo-TEM. Therefore, we combined high-power laser illumination and *in situ* visualization using confocal microscopy to directly observe photoinduced disassembly of a broad variety of giant dendrimersomes of distinct morphotypes and dynamic release of molecular and macromolecular cargos. We also observed spontaneous reassembly of lamellar and other nanoscale components, which may partially explain incomplete release of cargo from carriers reported by other laboratories.[30,37−42,60,61] By leveraging the multilamellar structure of dendrimersomes and an NTA Janus dendrimer, we developed a generalizable optical cargo release and recruitment platform that can be readily functionalized with His-tagged proteins that are commonly available in bioscience laboratories. The physicochemical mechanisms that underlie the morphological transformation of these dendrimersomes upon photocleavage is an important area for future study. Together, this versatile platform helps illuminate problems and challenges related to the molecular design of nanocarriers[62−68] and reveals alternative paradigms for photoregulation of and component release from vesicle-based carriers.

METHODS

Chemical Reagents. All reagents were obtained from commercial sources and used without purification unless otherwise stated. CH_2Cl_2 (DCM) was dried over CaH_2 and freshly distilled before use. THF was distilled over Na/benzophenone immediately before use. DMF was dried from CaH_2, distilled, and kept over molecular sieves prior to use. Solvents and reagents were deoxygenated when necessary by purging with nitrogen.

UV Photocleavage of Molecules. To monitor and analyze the products of photocleavage of Janus dendrimers, two UV illumination strategies were used. First, we tested a UV curing lamp ($\lambda_{max} \approx 365$ nm) equipped with two 8 W bulbs.[69] The sample solution in a 5 mL glass vial was placed under the lamp at a distance of 5 cm. Using this strategy and monitoring product formation *via* NMR, we determined the half-time to be <4 h. We reasoned that cleavage could be carried out much more quickly and therefore tested a second illumination strategy using more focused light. We illuminated wells containing 0.5 mL of dendrimer molecules in chloroform in a Labtek eight-well chamber using a Mercury lamp with a DAPI filter set, focusing the light through a 20× air objective on an Olympus IX81 inverted fluorescence microscope. To illuminate the entire well, we used the scan slide plugin in Metamorph software, exposing each image frame to 0.6 s of illumination and repeating the scan to achieve total illumination durations ranging from 1 to 21 min. For example, a 25 × 25 scan area (625 frames) with 0.6 s/frame illumination received 375 total seconds of exposure (6.25 min). Ultimately this strategy enabled 50% cleavage in just minutes.

NMR. ^1H and ^{13}C NMR spectra were recorded at 500 and 126 MHz respectively, on a Bruker DRX (500 MHz) NMR spectrometer. All NMR spectra were measured at 23 °C in $CDCl_3$ or d_4-CD_3OD. Chemical shifts (δ) are reported in ppm, and coupling constants (J) are reported in hertz (Hz). The resonance multiplicities in the ^1H NMR spectra are described as "s" (singlet), "d" (doublet), "t" (triplet), "quint" (quintet), and "m" (multiplet), and broad resonances are indicated by "br". Residual protic solvents of $CDCl_3$ (^1H, δ 7.26 ppm, ^{13}C, δ 77.16 ppm), d_4-CD_3OD (^1H, δ 3.35 ppm), and tetramethylsilane (TMS, δ 0 ppm) were used as the internal reference in the ^1H and ^{13}C NMR spectra. The absorptions are given in wavenumbers (cm^{-1}). NMR spectra were analyzed and exported by TopSpin 4.07 (Bruker).

Chromatography. Evolution of the photocleavage reaction was monitored by thin-layer chromatography (TLC) using silica gel 60 F_{254} precoated plates (E. Merck), and compounds were visualized by UV light with a wavelength of 254 or 356 nm. Purifications by flash column chromatography were performed using flash silica gel from Silicycle (60 Å, 40−63 μm) with the indicated eluent. The purity of the products was determined by a combination of TLC and high-pressure liquid chromatography (HPLC) using a Shimadzu LC-20AD high-performance liquid chromatograph pump, a PE Nelson Analytical 900 Series integration data station, a Shimadzu SPD-10A VP (UV−vis, λ = 254 nm), and three AM gel columns (a guard column, two 500 Å, 10 μm columns). THF was used as solvent at the oven temperature of 23 °C. Detection was carried out at a UV absorbance of 254 nm.

MALDI-TOF Mass Spectrometry. This was performed on a PerSeptive Biosystem-Voyager-DE (Framingham, MA, USA) mass spectrometer equipped with a nitrogen laser (337 nm) and operating in linear mode. Internal calibration was performed using angiotensin II and bombesin as standards. The analytical sample was obtained by mixing the THF solution of the sample (5−10 mg/mL) and THF solution of the matrix (2,5-dihydroxybenzoic acid, 10 mg/mL) in a 1:5 (v/v) ratio. The prepared solution of the sample and the matrix (0.5 μL) was loaded on the MALDI plate and allowed to dry at 23 °C

https://dx.doi.org/10.1021/acsnano.0c02912
ACS Nano XXXX, XXX, XXX−XXX

before the plate was inserted into the vacuum chamber of the MALDI instrument. The laser steps and voltages applied were adjusted depending on both the molecular weight and the nature of each analyzed compound.

Liquid Chromatography Mass Spectrometry (LCMS). After photocleavage, the Janus dendrimer sample was further diluted to ~0.01 mg/mL with acetonitrile and transferred into an autosampler vial, and 20 μL was injected into an HPLC-MS/MS system (a Waters ACQUITY UPLC system was used for chromatography). The UPLC column was 2.1 × 50 mm with 1.7 mm particles (Waters ACQUITY UPLC CSH C18). The mobile phase A was generated from water. The mobile phase B was made of acetonitrile−methanol, 95:5 (v/v), containing 0.1% formic acid. The flow rate was 350 μL/min. Separations were carried out with a linear solvent gradient starting from 0% B to 100% B over 5 min. The Waters Xevo TQS instrument (Waters Corporation) equipped with a triple quadrupole analyzer was operated in positive-mode ESI. The analyzer was set in the MS scan mode and daughter ion scan mode for the analysis.

Preparation of Nanoscale Dendrimersomes by Injection. Stock solutions were prepared by dissolving the amphiphilic Janus dendrimers in THF at 10 mg/mL. Dendrimersomes were then generated by injection of 50 μL of THF stock solution into 1.0 mL of mili-Q water, followed by 5 s of vortexing.

Dynamic Light Scattering. DLS for the monodisperse vesicles was performed in PBS and in Milli-Q water with a Malvern Instruments particle sizer (Zetasizer Nano S, Malvern Instruments, UK) equipped with 4 mW He−Ne laser 633 nm and avalanche photodiode positioned at 175° to the beam and temperature-controlled cuvette holder. Instrument parameters were determined automatically along with measurement times.

Cryogenic Transmission Electron Microscopy. Cryo-TEM micrographs were taken on a Carl Zeiss Libra 120 microscope. Cryo-TEM samples were prepared by plunge freezing an aqueous dispersion on plasma-treated lacey grids. The vitrified specimens were transferred to a Gatan-910 cryoholder. The images were recorded at a temperature of −170 °C with an acceleration voltage of 120 kV.

Preparation of Giant Dendrimersomes by Film Hydration. A mixture of a 50 μL chloroform solution containing photocleavable amphiphilic Janus dendrimers (10 mg/mL) and 2 μL of chloroform solution of red (rhodamine)-labeled Janus dendrimer **(3,5)12G1-RhB** (1 mg/mL) or green (nitrobenzoxadiazole)-labeled Janus dendrimer **(3,5)12G1-NBD** (1 mg/mL) was dried on a roughened Teflon sheet (0.5 × 0.5 cm^2) overnight by vacuum. Vesicles contained a final concentration of 0.4% w/w fluorescent tracer for imaging. After complete solvent evaporation, the films were rehydrated in 250 μL of milli-Q water or 1× phosphate-buffered saline (PBS) at 50 °C overnight. For the dendrimersomes encapsulated with Bodipy or Doxo rubicin, 1 mM Bodipy or Doxo was added during the hydration process. For dendrimersomes encapsulating DHFR enzyme, 10 μm of protein was added to 1× PBS and the film was hydrated at 37 °C overnight. Dendrimersomes containing NTA-dendrimer at 4% molar mass were first hydrated in milli-Q water at 50 °C overnight to ensure the dendrimers were well-mixed and then subsequently incubated with His-tagged proteins (His-RFP) at 10 μm for 30 min at room temperature. Samples were then diluted by 20−40-fold and imaged. For photoinduced protein recruitment, NTA-containing dendrimersomes were mixed with His-tagged protein, diluted to a final concentration of 0.2 μM.

Protein Expression and Purification. Recombinant plasmids for His-RFP and GST-DHFR-GFP were inducibly expressed in 1 L of bacterial cultures following transformation into Rosetta 2 BL21(DE3) pLysS *E. coli* strain (Novagen), as described previously.[70,71] After cell lysis *via* free-thaw and sonication, lysates were clarified by centrifugation and incubated with affinity resins to purify proteins. Lysates containing *E. coli* dihydrofolate reductase (DHFR) with an N-terminal fusion to glutathione-*S*-transferase (GST) and green fluorescence protein (GFP) were bound to glutathione agarose beads (Pierce) and pure protein eluted using 15 mM reduced glutathione, as described previously.[70] His-RFP-containing lysates were bound to Ni-NTA-Superflow beads (Qiagen) and eluted using 250 mM imidazole, as described previously.[71] Proteins were dialyzed and stored in a standard protein buffer (150 mM NaCl, 25 mM Tris-pH 7.8, 10% glycerol, 1 mM TCEP) at concentrations of 50−200 μM. Aliquots of protein that were flash frozen and stored in a −80C freezer were thawed and diluted to appropriate concentration (10 μm) prior to the start of the experiment. Protein concentrations were determined using Bradford Plus protein reagent and absorbance at 595 nm.

Confocal Fluorescence Microscopy. For confocal imaging experiments, samples of preassembled giant dendrimersomes were diluted 25−50-fold in milli-Q water to reduce background fluorescence and pipetted into custom gasket imaging chambers (20 μL). Images were acquired using 488 and 561 nm laser illumination on an Olympus IX81 inverted confocal microscope containing a Yokogawa X1 spinning disk head. Images were acquired using a 100× 1.4 NA oil objective, an Andor iXon3 EM-CCD camera, and MetaMorph acquisition software. Images containing a specific dye or tracer were collected at identical laser intensities and camera gain and exposed for the same period of time.

Laser Breakdown of Dendrimersome Vesicles. Rapid optical breakdown of giant dendrimersome samples was achieved *via* 405 nm laser illumination at either 1.66 or 2.74 mW power settings (corresponding to power densities at the center of 10 μm diameter vesicles, I = 34,583 and 57,083 mW/cm^2). Time-course experiments were performed at 1.66 mW laser power using a single plane of illumination in the widest plane of the vesicle; pulses were 20 ms in duration and repeated for an integrated total 405 nm exposure of 1−2 s. Cargo release experiments were performed by illumination of 20 planes along the Z-axis for a combined 5 s of 405 nm illumination, 1.66 mW power. This stack illumination strategy was repeated for up to a total of 20 s combined illumination. Photorelease of the outer vesicle layer was performed by stack illumination for a combined 1 s of 405 nm illumination, split between 20 z-planes. For targeted illumination of regions of interest, such as to alter vesicle morphology, a Gataca Systems ILAS2 targeted laser was used containing galvanometer scan heads. Regions of approximately 1 μm^2 were illuminated at 10 repetitions for a combined 40−80 ms of 405 nm exposure.

Image Analysis. To categorize vesicles based on their morphology, individual vesicles were manually contoured at their midplane using ImageJ software and grouped into three main categories: unilameller-like (≤2 visible lamellae), onion-like (multi-lamellar), and dense vesicles. A total of 573 vesicles for four types of photocleavable dendrimers were used. Additionally, a total of 113 vesicles of nonphotocleavable dendrimers across three imaging sessions were included to account for dendrimersome and experiment variability. The vast majority of vesicles were round, and thus their mean diameter was calculated from the measured area. To quantify kinetics of vesicle breakdown, extent of cargo release, and amount of protein recruitment, confocal image stacks were analyzed using ImageJ. Midplanes of vesicle or vesicle breakdown products were identified in Z, and objects were masked and background subtracted to calculate integrated pixel intensities of fluorescent dendrimers or small molecule or macromolecular cargos. Masking area of breakdown products included all visible debris field using a fluorescent dendrimer tracer; the area was confirmed by the 405 nm channel, which shows absorption of the nitrobenzyl group. Measurements of breakdown or recruitment were performed on a minimum of 20−25 vesicles. Analyses of control experiments containing photoinsensitive dendrimersomes included at least 10 vesicles. Analyses of time required to form observable breaks in lamellae were performed on timelapse image stacks using the Rho-dendrimer channel. All data were plotted and fit using Graphpad Prism software. Statistical calculations, including nonparametric two-tailed t tests of statistical significance and comparison of linear regression slopes, were performed in Prism.

https://dx.doi.org/10.1021/acsnano.0c02912
ACS Nano XXXX, XXX, XXX−XXX

ASSOCIATED CONTENT

Supporting Information

The Supporting Information is available free of charge at https://pubs.acs.org/doi/10.1021/acsnano.0c02912.

Supplemental movie (AVI)
Supplemental movie (AVI)
Supplemental movie (AVI)
Supplemental movie (AVI)
Supplemental movie (AVI)
Supplemental movie (AVI)
Synthetic procedures with complete data characterization, supplemental Figures S1−S13, and supplemental references (PDF)

AUTHOR INFORMATION

Corresponding Authors

Virgil Percec − *Roy & Diana Vagelos Laboratories, Department of Chemistry, University of Pennsylvania, Philadelphia, Pennsylvania 19104-6323, United States;* orcid.org/0000-0001-5926-0489; Email: percec@sas.upenn.edu

Matthew C. Good − *Department of Cell and Developmental Biology, Perelman School of Medicine and Department of Bioengineering, University of Pennsylvania, Philadelphia, Pennsylvania 19104-6058, United States;* orcid.org/0000-0002-6367-1034; Email: mattgood@pennmedicine.upenn.edu

Authors

Shangda Li − *Roy & Diana Vagelos Laboratories, Department of Chemistry, University of Pennsylvania, Philadelphia, Pennsylvania 19104-6323, United States*

Boao Xia − *Department of Cell and Developmental Biology, Perelman School of Medicine, University of Pennsylvania, Philadelphia, Pennsylvania 19104-6058, United States*

Bilal Javed − *Roy & Diana Vagelos Laboratories, Department of Chemistry, University of Pennsylvania, Philadelphia, Pennsylvania 19104-6323, United States*

William D. Hasley − *Roy & Diana Vagelos Laboratories, Department of Chemistry, University of Pennsylvania, Philadelphia, Pennsylvania 19104-6323, United States*

Adriel Melendez-Davila − *Roy & Diana Vagelos Laboratories, Department of Chemistry, University of Pennsylvania, Philadelphia, Pennsylvania 19104-6323, United States*

Matthew Liu − *Roy & Diana Vagelos Laboratories, Department of Chemistry, University of Pennsylvania, Philadelphia, Pennsylvania 19104-6323, United States*

Meir Kerzner − *Roy & Diana Vagelos Laboratories, Department of Chemistry, University of Pennsylvania, Philadelphia, Pennsylvania 19104-6323, United States*

Shriya Agarwal − *Roy & Diana Vagelos Laboratories, Department of Chemistry, University of Pennsylvania, Philadelphia, Pennsylvania 19104-6323, United States*

Qi Xiao − *Roy & Diana Vagelos Laboratories, Department of Chemistry, University of Pennsylvania, Philadelphia, Pennsylvania 19104-6323, United States; Institute of Computational Molecular Science, Temple University, Philadelphia, Pennsylvania 19122, United States;* orcid.org/0000-0002-6470-0407

Paola Torre − *Department of Cell and Developmental Biology, Perelman School of Medicine, University of Pennsylvania, Philadelphia, Pennsylvania 19104-6058, United States*

Jessica G. Bermudez − *Department of Bioengineering, University of Pennsylvania, Philadelphia, Pennsylvania 19104-6321, United States*

Khosrow Rahimi − *DWI−Leibniz Institute for Interactive Materials, 52074 Aachen, Germany; Institute of Technical and Macromolecular Chemistry, RWTH Aachen University, 52074 Aachen, Germany;* orcid.org/0000-0002-1865-0808

Nina Yu. Kostina − *DWI−Leibniz Institute for Interactive Materials, 52074 Aachen, Germany; Institute of Technical and Macromolecular Chemistry, RWTH Aachen University, 52074 Aachen, Germany*

Martin Möller − *DWI−Leibniz Institute for Interactive Materials, 52074 Aachen, Germany; Institute of Technical and Macromolecular Chemistry, RWTH Aachen University, 52074 Aachen, Germany;* orcid.org/0000-0002-5955-4185

Cesar Rodriguez-Emmenegger − *DWI−Leibniz Institute for Interactive Materials, 52074 Aachen, Germany; Institute of Technical and Macromolecular Chemistry, RWTH Aachen University, 52074 Aachen, Germany;* orcid.org/0000-0003-0745-0840

Michael L. Klein − *Institute of Computational Molecular Science, Temple University, Philadelphia, Pennsylvania 19122, United States*

Complete contact information is available at: https://pubs.acs.org/10.1021/acsnano.0c02912

Notes

The authors declare no competing financial interest.

ACKNOWLEDGMENTS

This work was supported by National Science Foundation Grants DMR-1807127 (V.P.) and DMR-1720530 (to M.C.G. and V.P.); the P. Roy Vagelos Chair at the University of Pennsylvania (V.P.); the Alexander von Humboldt Foundation (to N.Y.K. and V.P.); Burroughs Welcome Fund (M.C.G.); Department of Energy DE-SC0007063 (M.C.G.), NSF Superseed (M.C.G.); Sheikh Saqr Research Foundation (to M.L.K.); and the European Union's Horizon H2020- NMBP-TR-IND-2018, EVPRO (Development of Extracellular Vesicles loaded hydrogel coatings with immunomodulatory activity for Promoted Regenerative Osseointegration of revision endoprosthesis) grant 814495-2 (to C.R.-E. and N.Y.K.). Funding by the European Commission within the ERC - Advanced Grant 695716 "Jellyclock" (M.M) is acknowledged. We thank the Cell and Developmental Biology Microscopy Core in the Perelman School of Medicine.

REFERENCES

(1) Luisi, P. L. *The Emergence of Life: From Chemical Origins to Synthetic Biology*, 2nd ed.; Cambridge University Press: Cambridge, UK, 2016; pp 263−399.

(2) Hanczyc, M. M.; Szostak, J. W. Replicating Vesicles as Models of Primitive Cell Growth and Division. *Curr. Opin. Chem. Biol.* **2004**, *8*, 660−664.

(3) Mansy, S. S.; Schrum, J. P.; Krishnamurthy, M.; Tobé, S.; Treco, D. A.; Szostak, J. W. Template-Directed Synthesis of a Genetic Polymer in a Model Protocell. *Nature* **2008**, *454*, 122−125.

(4) Schwille, P.; Spatz, J.; Landfester, K.; Bodenschatz, E.; Herminghaus, S.; Sourjik, V.; Erb, T. J.; Bastiaens, P.; Lipowsky, R.; Hyman, A.; Dabrock, P.; Baret, J.-C.; Vidakovic-Koch, T.; Bieling, P.; Dimova, R.; Mutschler, H.; Robinson, T.; Tang, T. Y. D.; Wegner, S.; Sundmacher, K. Maxsynbio: Avenues Towards Creating Cells from the Bottom Up. *Angew. Chem., Int. Ed.* **2018**, *57*, 13382−13392.

https://dx.doi.org/10.1021/acsnano.0c02912
ACS Nano XXXX, XXX, XXX−XXX

(5) Brea, R. J.; Hardy, M. D.; Devaraj, N. K. Towards Self-Assembled Hybrid Artificial Cells: Novel Bottom-Up Approaches to Functional Synthetic Membranes. *Chem. - Eur. J.* **2015**, *21*, 12564−12570.
(6) Allen, T. M.; Cullis, P. R. Drug Delivery Systems: Entering the Mainstream. *Science* **2004**, *303*, 1818−1822.
(7) Pattni, B. S.; Chupin, V. V.; Torchilin, V. P. New Developments in Liposomal Drug Delivery. *Chem. Rev.* **2015**, *115*, 10938−10966.
(8) Torchilin, V. P. Multifunctional Nanocarriers. *Adv. Drug Delivery Rev.* **2012**, *64*, 302−315.
(9) Torchilin, V. P. Recent Advances with Liposomes as Pharmaceutical Carriers. *Nat. Rev. Drug Discovery* **2005**, *4*, 145−160.
(10) Cheng, Z.; Zaki, A. A.; Hui, J. Z.; Muzykantov, V. R.; Tsourkas, A. Multifunctional Nanoparticles: Cost *Versus* Benefit of Adding Targeting and Imaging Capabilities. *Science* **2012**, *338*, 903−910.
(11) Barenholz, Y. Liposome Application: Problems and Prospects. *Curr. Opin. Colloid Interface Sci.* **2001**, *6*, 66−77.
(12) Taylor, T. M.; Davidson, P. M.; Bruce, B. D.; Weiss, J. Liposomal Nanocapsules in Food Science and Agriculture. *Crit. Rev. Food Sci. Nutr.* **2005**, *45*, 587−605.
(13) Patravale, V. B.; Mandawgade, S. D. Novel Cosmetic Delivery Systems: An Application Update. *Int. J. Cosmet. Sci.* **2008**, *30*, 19−33.
(14) Bangham, A. D.; Standish, M. M.; Watkins, J. C. Diffusion of Univalent Ions across the Lamellae of Swollen Phospholipids. *J. Mol. Biol.* **1965**, *13*, 238−252.
(15) Guo, X.; Szoka, F. C., Jr. Chemical Approaches to Triggerable Lipid Vesicles for Drug and Gene Delivery. *Acc. Chem. Res.* **2003**, *36*, 335−341.
(16) Ringsdorf, H.; Schlarb, B.; Venzmer, J. Molecular Architecture and Function of Polymeric Oriented Systems: Models for the Study of Organization, Surface Recognition, and Dynamics of Biomembranes. *Angew. Chem., Int. Ed. Engl.* **1988**, *27*, 113−158.
(17) Discher, B. M.; Won, Y.-Y.; Ege, D. S.; Lee, J. C. M.; Bates, F. S.; Discher, D. E.; Hammer, D. A. Polymersomes: Tough Vesicles Made from Diblock Copolymers. *Science* **1999**, *284*, 1143−1146.
(18) Discher, D. E.; Ortiz, V.; Srinivas, G.; Klein, M. L.; Kim, Y.; Christian, D.; Cai, S.; Photos, P.; Ahmed, F. Emerging Applications of Polymersomes in Delivery: From Molecular Dynamics to Shrinkage of Tumors. *Prog. Polym. Sci.* **2007**, *32*, 838−857.
(19) Rodriguez, A. R.; Choe, U.-J.; Kamei, D. T.; Deming, T. J. Blending of Diblock and Triblock Copolypeptide Amphiphiles Yields Cell Penetrating Vesicles with Low Toxicity. *Macromol. Biosci.* **2015**, *15*, 90−97.
(20) Percec, V.; Wilson, D. A.; Leowanawat, P.; Wilson, C. J.; Hughes, A. D.; Kaucher, M. S.; Hammer, D. A.; Levine, D. H.; Kim, A. J.; Bates, F. S.; Davis, K. P.; Lodge, T. P.; Klein, M. L.; DeVane, R. H.; Aqad, E.; Rosen, B. M.; Argintaru, A. O.; Sienkowska, M. J.; Rissanen, K.; Nummelin, S.; et al. Self-Assembly of Janus Dendrimers into Uniform Dendrimersomes and Other Complex Architectures. *Science* **2010**, *328*, 1009−1014.
(21) Sherman, S. E.; Xiao, Q.; Percec, V. Mimicking Complex Biological Membranes and Their Programmable Glycan Ligands with Dendrimersomes and Glycodendrimersomes. *Chem. Rev.* **2017**, *117*, 6538−6631.
(22) Barnard, A.; Posocco, P.; Pricl, S.; Calderon, M.; Haag, R.; Hwang, M. E.; Shum, V. W.; Pack, D. W.; Smith, D. K. Degradable Self-Assembling Dendrons for Gene Delivery: Experimental and Theoretical Insights into the Barriers to Cellular Uptake. *J. Am. Chem. Soc.* **2011**, *133*, 20288−20300.
(23) Kostiainen, M. A.; Smith, D. K.; Ikkala, O. Optically Triggered Release of DNA from Multivalent Dendrons by Degrading and Charge-Switching Multivalency. *Angew. Chem., Int. Ed.* **2007**, *46*, 7600−7604.
(24) Mogaki, R.; Okuro, K.; Ueki, R.; Sando, S.; Aida, T. Molecular Glue That Spatiotemporally Turns on Protein-Protein Interactions. *J. Am. Chem. Soc.* **2019**, *141*, 8035−8040.
(25) Torre, P.; Xiao, Q.; Buzzacchera, I.; Sherman, S. E.; Rahimi, K.; Kostina, N. Y.; Rodriguez-Emmenegger, C.; Möller, M.; Wilson, C. J.; Klein, M. L.; Good, M. C.; Percec, V. Encapsulation of Hydrophobic Components in Dendrimersomes and Decoration of Their Surface with Proteins and Nucleic Acids. *Proc. Natl. Acad. Sci. U. S. A.* **2019**, *116*, 15378−15385.
(26) Xiao, Q.; Yadavalli, S. S.; Zhang, S.; Sherman, S. E.; Fiorin, E.; Silva, L. d.; Wilson, D. A.; Hammer, D. A.; André, S.; Gabius, H.-J.; Klein, M. L.; Goulian, M.; Percec, V. Bioactive Cell-Like Hybrids Coassembled from (Glyco)Dendrimersomes with Bacterial Membranes. *Proc. Natl. Acad. Sci. U. S. A.* **2016**, *113*, E1134−E1141.
(27) Yadavalli, S. S.; Xiao, Q.; Sherman, S. E.; Hasley, W. D.; Klein, M. L.; Goulian, M.; Percec, V. Bioactive Cell-Like Hybrids from Dendrimersomes with a Human Cell Membrane and Its Components. *Proc. Natl. Acad. Sci. U. S. A.* **2019**, *116*, 744−752.
(28) Kostina, N. Y.; Rahimi, K.; Xiao, Q.; Haraszti, T.; Dedisch, S.; Spatz, J. P.; Schwaneberg, U.; Klein, M. L.; Percec, V.; Möller, M.; Rodriguez-Emmenegger, C. Membrane-Mimetic Dendrimersomes Engulf Living Bacteria *Via* Endocytosis. *Nano Lett.* **2019**, *19*, 5732−5738.
(29) Duan, Q.; Cao, Y.; Li, Y.; Hu, X.; Xiao, T.; Lin, C.; Pan, Y.; Wang, L. pH-Responsive Supramolecular Vesicles Based on Water-Soluble Pillar[6]Arene and Ferrocene Derivative for Drug Delivery. *J. Am. Chem. Soc.* **2013**, *135*, 10542−10549.
(30) Gillies, E. R.; Fréchet, J. M. J. pH-Responsive Copolymer Assemblies for Controlled Release of Doxorubicin. *Bioconjugate Chem.* **2005**, *16*, 361−368.
(31) Kanamala, M.; Wilson, W. R.; Yang, M.; Palmer, B. D.; Wu, Z. Mechanisms and Biomaterials in pH-Responsive Tumour Targeted Drug Delivery: A Review. *Biomaterials* **2016**, *85*, 152−167.
(32) Chang, Y.; Yang, K.; Wei, P.; Huang, S.; Pei, Y.; Zhao, W.; Pei, Z. Cationic Vesicles Based on Amphiphilic Pillar[5]Arene Capped with Ferrocenium: A Redox-Responsive System for Drug/Sirna Co-Delivery. *Angew. Chem., Int. Ed.* **2014**, *53*, 13126−13130.
(33) Meng, F.; Hennink, W. E.; Zhong, Z. Reduction-Sensitive Polymers and Bioconjugates for Biomedical Applications. *Biomaterials* **2009**, *30*, 2180−2198.
(34) Ong, W.; Yang, Y.; Cruciano, A. C.; McCarley, R. L. Redox-Triggered Contents Release from Liposomes. *J. Am. Chem. Soc.* **2008**, *130*, 14739−14744.
(35) Gohy, J.-F.; Zhao, Y. Photo-Responsive Block Copolymer Micelles: Design and Behavior. *Chem. Soc. Rev.* **2013**, *42*, 7117−7129.
(36) Katz, J. S.; Zhong, S.; Ricart, B. G.; Pochan, D. J.; Hammer, D. A.; Burdick, J. A. Modular Synthesis of Biodegradable Diblock Copolymers for Designing Functional Polymersomes. *J. Am. Chem. Soc.* **2010**, *132*, 3654−3655.
(37) Nazemi, A.; Gillies, E. R. Dendrimersomes with Photodegradable Membranes for Triggered Release of Hydrophilic and Hydrophobic Cargo. *Chem. Commun.* **2014**, *50*, 11122−11125.
(38) Yesilyurt, V.; Ramireddy, R.; Thayumanavan, S. Photoregulated Release of Noncovalent Guests from Dendritic Amphiphilic Nanocontainers. *Angew. Chem., Int. Ed.* **2011**, *50*, 3038−3042.
(39) Dong, J.; Xun, Z.; Zeng, Y.; Yu, T.; Han, Y.; Chen, J.; Li, Y.-Y.; Yang, G.; Li, Y. A Versatile and Robust Vesicle Based on a Photocleavable Surfactant for Two-Photon-Tuned Release. *Chem. - Eur. J.* **2013**, *19*, 7931−7936.
(40) Zhang, W.-J.; Hong, C.-Y.; Pan, C.-Y. Efficient Fabrication of Photosensitive Polymeric Nano-Objects *Via* an Ingenious Formulation of Raft Dispersion Polymerization and Their Application for Drug Delivery. *Biomacromolecules* **2017**, *18*, 1210−1217.
(41) Molla, M. R.; Rangadurai, P.; Antony, L.; Swaminathan, S.; de Pablo, J. J.; Thayumanavan, S. Dynamic Actuation of Glassy Polymersomes through Isomerization of a Single Azobenzene Unit at the Block Copolymer Interface. *Nat. Chem.* **2018**, *10*, 659−666.
(42) Fomina, N.; Sankaranarayanan, J.; Almutairi, A. Photochemical Mechanisms of Light-Triggered Release from Nanocarriers. *Adv. Drug Delivery Rev.* **2012**, *64*, 1005−1020.
(43) Percec, V.; Leowanawat, P.; Sun, H.-J.; Kulikov, O.; Nusbaum, C. D.; Tran, T. M.; Bertin, A.; Wilson, D. A.; Peterca, M.; Zhang, S.; Kamat, N. P.; Vargo, K.; Moock, D.; Johnston, E. D.; Hammer, D. A.; Pochan, D. J.; Chen, Y.; Chabre, Y. M.; Shiao, T. C.; Bergeron-Brlek, M.; et al. Modular Synthesis of Amphiphilic Janus Glycodendrimers

https://dx.doi.org/10.1021/acsnano.0c02912
ACS Nano XXXX, XXX, XXX−XXX

and Their Self-Assembly into Glycodendrimersomes and Other Complex Architectures with Bioactivity to Biomedically Relevant Lectins. *J. Am. Chem. Soc.* **2013**, *135*, 9055−9077.
(44) Zhang, S.; Sun, H.-J.; Hughes, A. D.; Draghici, B.; Lejnieks, J.; Leowanawat, P.; Bertin, A.; Otero De Leon, L.; Kulikov, O. V.; Chen, Y.; Pochan, D. J.; Heiney, P. A.; Percec, V. Single−Single" Amphiphilic Janus Dendrimers Self-Assemble into Uniform Dendrimersomes with Predictable Size. *ACS Nano* **2014**, *8*, 1554−1565.
(45) Rodriguez-Emmenegger, C.; Xiao, Q.; Kostina, N. Y.; Sherman, S. E.; Rahimi, K.; Partridge, B. E.; Li, S.; Sahoo, D.; Reveron Perez, A. M.; Buzzacchera, I.; Han, H.; Kerzner, M.; Malhotra, I.; Möller, M.; Wilson, C. J.; Good, M. C.; Goulian, M.; Baumgart, T.; Klein, M. L.; Percec, V. Encoding Biological Recognition in a Bicomponent Cell-Membrane Mimic. *Proc. Natl. Acad. Sci. U. S. A.* **2019**, *116*, 5376−5382.
(46) Xiao, Q.; Zhang, S.; Wang, Z.; Sherman, S. E.; Moussodia, R.-O.; Peterca, M.; Muncan, A.; Williams, D. R.; Hammer, D. A.; Vértesy, S.; André, S.; Gabius, H.-J.; Klein, M. L.; Percec, V. Onion-Like Glycodendrimersomes from Sequence-Defined Janus Glycodendrimers and Influence of Architecture on Reactivity to a Lectin. *Proc. Natl. Acad. Sci. U. S. A.* **2016**, *113*, 1162−1167.
(47) Zhang, S.; Xiao, Q.; Sherman, S. E.; Muncan, A.; Ramos Vicente, A. D. M.; Wang, Z.; Hammer, D. A.; Williams, D.; Chen, Y.; Pochan, D. J.; Vértesy, S.; André, S.; Klein, M. L.; Gabius, H.-J.; Percec, V. Glycodendrimersomes from Sequence-Defined Janus Glycodendrimers Reveal High Activity and Sensor Capacity for the Agglutination by Natural Variants of Human Lectins. *J. Am. Chem. Soc.* **2015**, *137*, 13334−13344.
(48) Xiao, Q.; Ludwig, A.-K.; Romanò, C.; Buzzacchera, I.; Sherman, S. E.; Vetro, M.; Vértesy, S.; Kaltner, H.; Reed, E. H.; Möller, M.; Wilson, C. J.; Hammer, D. A.; Oscarson, S.; Klein, M. L.; Gabius, H.-J.; Percec, V. Exploring Functional Pairing between Surface Glycoconjugates and Human Galectins Using Programmable Glycodendrimersomes. *Proc. Natl. Acad. Sci. U. S. A.* **2018**, *115*, E2509−E2518.
(49) Bochet, C. G. Photolabile Protecting Groups and Linkers. *J. Chem. Soc., Perkin Trans. 1* **2002**, 125−142.
(50) Dong, J.; Zeng, Y.; Xun, Z.; Han, Y.; Chen, J.; Li, Y.-Y.; Li, Y. Stabilized Vesicles Consisting of Small Amphiphiles for Stepwise Photorelease *Via* Uv Light. *Langmuir* **2012**, *28*, 1733−1737.
(51) Rich, D. H.; Gurwara, S. K. Preparation of a New O-Nitrobenzyl Resin for Solid-Phase Synthesis of Tert-Butyloxycarbonyl-Protected Peptide Acids. *J. Am. Chem. Soc.* **1975**, *97*, 1575−1579.
(52) Yu, Z.-Q.; Xu, X.-M.; Hong, C.-Y.; Wu, D.-C.; You, Y.-Z. A Responsive Hyperbranched Polymer Not Only Can Self-Immolate but Also Can Self-Cross-Link. *Macromolecules* **2014**, *47*, 4136−4143.
(53) Gruner, S. M.; Lenk, R. P.; Janoff, A. S.; Ostro, M. J. Novel Multilayered Lipid Vesicles: Comparison of Physical Characteristics of Multilamellar Liposomes and Stable Plurilamellar Vesicles. *Biochemistry* **1985**, *24*, 2833−2842.
(54) Bagatolli, L. A.; Parasassi, T.; Gratton, E. Giant Phospholipid Vesicles: Comparison among the Whole Lipid Sample Characteristics Using Different Preparation Methods: A Two Photon Fluorescence Microscopy Study. *Chem. Phys. Lipids* **2000**, *105*, 135−147.
(55) Sezgin, E.; Schwille, P. Fluorescence Techniques to Study Lipid Dynamics. *Cold Spring Harbor Perspect. Biol.* **2011**, *3*, a009803.
(56) Xiao, Q.; Rubien, J. D.; Wang, Z.; Reed, E. H.; Hammer, D. A.; Sahoo, D.; Heiney, P. A.; Yadavalli, S. S.; Goulian, M.; Wilner, S. E.; Baumgart, T.; Vinogradov, S. A.; Klein, M. L.; Percec, V. Self-Sorting and Coassembly of Fluorinated, Hydrogenated, and Hybrid Janus Dendrimers into Dendrimersomes. *J. Am. Chem. Soc.* **2016**, *138*, 12655−12663.
(57) Zhang, S.; Sun, H.-J.; Hughes, A. D.; Moussodia, R.-O.; Bertin, A.; Chen, Y.; Pochan, D. J.; Heiney, P. A.; Klein, M. L.; Percec, V. Self-Assembly of Amphiphilic Janus Dendrimers into Uniform Onion-Like Dendrimersomes with Predictable Size and Number of Bilayers. *Proc. Natl. Acad. Sci. U. S. A.* **2014**, *111*, 9058−9063.
(58) Shrimpton, P.; Allemann, R. K. Role of Water in the Catalytic Cycle of *E* Coli Dihydrofolate Reductase. *Protein Sci.* **2002**, *11*, 1442−1451.
(59) Wilner, S. E.; Xiao, Q.; Graber, Z. T.; Sherman, S. E.; Percec, V.; Baumgart, T. Dendrimersomes Exhibit Lamellar-to-Sponge Phase Transitions. *Langmuir* **2018**, *34*, 5527−5534.
(60) Gillies, E. R. Reflections on the Evolution of Smart Polymers. *Isr. J. Chem.* **2020**, *60*, 75−85.
(61) Yardley, R. E.; Gillies, E. R. Multi-Stimuli-Responsive Self-Immolative Polymer Assemblies. *J. Polym. Sci., Part A: Polym. Chem.* **2018**, *56*, 1868−1877.
(62) Bellomo, E. G.; Wyrsta, M. D.; Pakstis, L.; Pochan, D. J.; Deming, T. J. Stimuli-Responsive Polypeptide Vesicles by Conformation-Specific Assembly. *Nat. Mater.* **2004**, *3*, 244−248.
(63) Cabral, H.; Miyata, K.; Osada, K.; Kataoka, K. Block Copolymer Micelles in Nanomedicine Applications. *Chem. Rev.* **2018**, *118*, 6844−6892.
(64) Farokhzad, O. C.; Langer, R. Impact of Nanotechnology on Drug Delivery. *ACS Nano* **2009**, *3*, 16−20.
(65) Kim, B.-S.; Park, S. W.; Hammond, P. T. Hydrogen-Bonding Layer-by-Layer-Assembled Biodegradable Polymeric Micelles as Drug Delivery Vehicles from Surfaces. *ACS Nano* **2008**, *2*, 386−392.
(66) Kloxin, A. M.; Kasko, A. M.; Salinas, C. N.; Anseth, K. S. Photodegradable Hydrogels for Dynamic Tuning of Physical and Chemical Properties. *Science* **2009**, *324*, 59−63.
(67) Rideau, E.; Dimova, R.; Schwille, P.; Wurm, F. R.; Landfester, K. Liposomes and Polymersomes: A Comparative Review Towards Cell Mimicking. *Chem. Soc. Rev.* **2018**, *47*, 8572−8610.
(68) Wei, T.; Chen, C.; Liu, J.; Liu, C.; Posocco, P.; Liu, X.; Cheng, Q.; Huo, S.; Liang, Z.; Fermeglia, M.; Pricl, S.; Liang, X.-J.; Rocchi, P.; Peng, L. Anticancer Drug Nanomicelles Formed by Self-Assembling Amphiphilic Dendrimer to Combat Cancer Drug Resistance. *Proc. Natl. Acad. Sci. U. S. A.* **2015**, *112*, 2978−2983.
(69) Anastasaki, A.; Nikolaou, V.; Zhang, Q.; Burns, J.; Samanta, S. R.; Waldron, C.; Haddleton, A. J.; McHale, R.; Fox, D.; Percec, V.; Wilson, P.; Haddleton, D. M. Copper(II)/Tertiary Amine Synergy in Photoinduced Living Radical Polymerization: Accelerated Synthesis of Omega-Functional and Alpha,Omega-Heterofunctional Poly(Acrylates). *J. Am. Chem. Soc.* **2014**, *136*, 1141−1149.
(70) Caldwell, R. M.; Bermudez, J. G.; Thai, D.; Aonbangkhen, C.; Schuster, B. S.; Courtney, T.; Deiters, A.; Hammer, D. A.; Chenoweth, D. M.; Good, M. C. Optochemical Control of Protein Localization and Activity within Cell-Like Compartments. *Biochemistry* **2018**, *57*, 2590−2596.
(71) Schuster, B. S.; Reed, E. H.; Parthasarathy, R.; Jahnke, C. N.; Caldwell, R. M.; Bermudez, J. G.; Ramage, H.; Good, M. C.; Hammer, D. A. Controllable Protein Phase Separation and Modular Recruitment to Form Responsive Membraneless Organelles. *Nat. Commun.* **2018**, *9*, 2985.

https://dx.doi.org/10.1021/acsnano.0c02912
ACS Nano XXXX, XXX, XXX−XXX